



## Neutron-rich nuclei produced at zero degrees in damped collisions induced by a beam of $^{18}\text{O}$ on a $^{238}\text{U}$ target



I. Stefan<sup>a,\*</sup>, B. Fornal<sup>b</sup>, S. Leoni<sup>c,d</sup>, F. Azaiez<sup>a,1</sup>, C. Portail<sup>a</sup>, J.C. Thomas<sup>e</sup>, A.V. Karpov<sup>i</sup>, D. Ackermann<sup>e</sup>, P. Bednarczyk<sup>b</sup>, Y. Blumenfeld<sup>a</sup>, S. Calinescu<sup>h</sup>, A. Chbihi<sup>e</sup>, M. Ciemala<sup>b</sup>, N. Cieplicka-Oryńczak<sup>b,d</sup>, F.C.L. Crespi<sup>c,d</sup>, S. Franchoo<sup>a</sup>, F. Hammache<sup>a</sup>, Ł.W. Iskra<sup>b</sup>, B. Jacquot<sup>e</sup>, R.V.F. Janssens<sup>f,2</sup>, O. Kamalou<sup>e</sup>, T. Lauritsen<sup>f</sup>, M. Lewitowicz<sup>e</sup>, L. Olivier<sup>a</sup>, S.M. Lukyanov<sup>i</sup>, M. Maccormick<sup>a</sup>, A. Maj<sup>b</sup>, P. Marini<sup>g,3</sup>, I. Matea<sup>a</sup>, M.A. Naumenko<sup>i</sup>, F. de Oliveira Santos<sup>e</sup>, C. Petrone<sup>h</sup>, Yu.E. Penionzhkevich<sup>i,k</sup>, F. Rotaru<sup>h</sup>, H. Savajols<sup>e</sup>, O. Sorlin<sup>e</sup>, M. Stanoiu<sup>h</sup>, B. Szpak<sup>b</sup>, O.B. Tarasov<sup>i,j</sup>, D. Verney<sup>a</sup>

<sup>a</sup> Institut de Physique Nucléaire, CNRS-IN2P3, Université Paris-Sud, Université Paris-Saclay, 91406 Orsay Cedex, France

<sup>b</sup> Institute of Nuclear Physics, PAN, 31-342 Kraków, Poland

<sup>c</sup> Dipartimento di Fisica, Università degli Studi di Milano, I-20133 Milano, Italy

<sup>d</sup> INFN sezione di Milano via Celoria 16, 20133, Milano, Italy

<sup>e</sup> GANIL, CEA/DRF-CNRS/IN2P3, Bvd Henri Becquerel, 14076 Caen, France

<sup>f</sup> Physics Division, Argonne National Laboratory, Argonne, IL 60439, USA

<sup>g</sup> CENBG, CNRS/IN2P3-Université de Bordeaux, 19 Chemin du Solarium, 33175 Gradignan, France

<sup>h</sup> Horia Hulubei National Institute for Physics and Nuclear Engineering, P.O. Box MG-6, 077125 Bucharest-Magurele, Romania

<sup>i</sup> Flerov Laboratory of Nuclear Reactions, JINR, 141980 Dubna, Russia

<sup>j</sup> National Superconducting Cyclotron Laboratory, Michigan State University, East Lansing, MI 48824, USA

<sup>k</sup> National Research Nuclear University MEPhI, Moscow, Russia

### ARTICLE INFO

#### Article history:

Received 27 November 2017

Received in revised form 3 February 2018

Accepted 16 February 2018

Available online 22 February 2018

Editor: V. Metag

#### Keywords:

Nuclear reactions

Deep-inelastic collisions

Exotic nuclei

### ABSTRACT

Cross sections and corresponding momentum distributions have been measured for the first time at zero degrees for the exotic nuclei obtained from a beam of  $^{18}\text{O}$  at 8.5 MeV/A impinging on a  $1\text{ mg/cm}^2\ ^{238}\text{U}$  target. Sizable cross sections were found for the production of exotic species arising from the neutron transfer and proton removal from the projectile. Comparisons of experimental results with calculations based on deep-inelastic reaction models, taking into account the particle evaporation process, indicate that zero degree is a scattering angle at which the differential reaction cross section for production of exotic nuclei is at its maximum. This result is important in view of the new generation of zero degrees spectrometers under construction, such as the S3 separator at GANIL, for example.

© 2018 The Author(s). Published by Elsevier B.V. This is an open access article under the CC BY license (<http://creativecommons.org/licenses/by/4.0/>). Funded by SCOAP<sup>3</sup>.

Deep-inelastic processes [1] between complex nuclei were first observed in the 1960s [2], but it was not until the early 1970s that the importance of such reaction mechanisms was recognized by experimental groups and that theoretical concepts were developed

(e.g., [3–6,1]) for their description. These processes acquired the name *deep-inelastic collisions*, or *damped collisions* or *multinucleon transfer* reactions. Characteristic features of deep-inelastic collisions (DIC) include: formation of a dinuclear system which rotates almost rigidly, exchange of nucleons governed by N/Z equilibration, damping of the relative kinetic energy between the reaction partners, transfer of relatively high angular momentum into the intrinsic spin of the reaction products, and, eventually, separation into two fragments. It has been known for a long time that projectile-like fragments (PLF) arising from the transfer of a few nucleons to or from the target are associated with short interaction times – they are emitted close to the grazing angle. In contrast, larger net nucleon transfers are associated with progressively longer interac-

\* Corresponding author.

E-mail address: [stefan@ipno.in2p3.fr](mailto:stefan@ipno.in2p3.fr) (I. Stefan).

<sup>1</sup> Present address: iThemba LABS, P.O. Box 722, Somerset West, 7129, South Africa.

<sup>2</sup> Present address: Dept. of Physics and Astronomy, University of North Carolina at Chapel Hill, Chapel Hill, North Carolina 27599-3255, USA and Triangle Universities Nuclear Laboratory, Duke University, Durham, North Carolina 27708-2308, USA.

<sup>3</sup> Present address: CEA, DAM, DIF, F-91297 Arpajon, France.

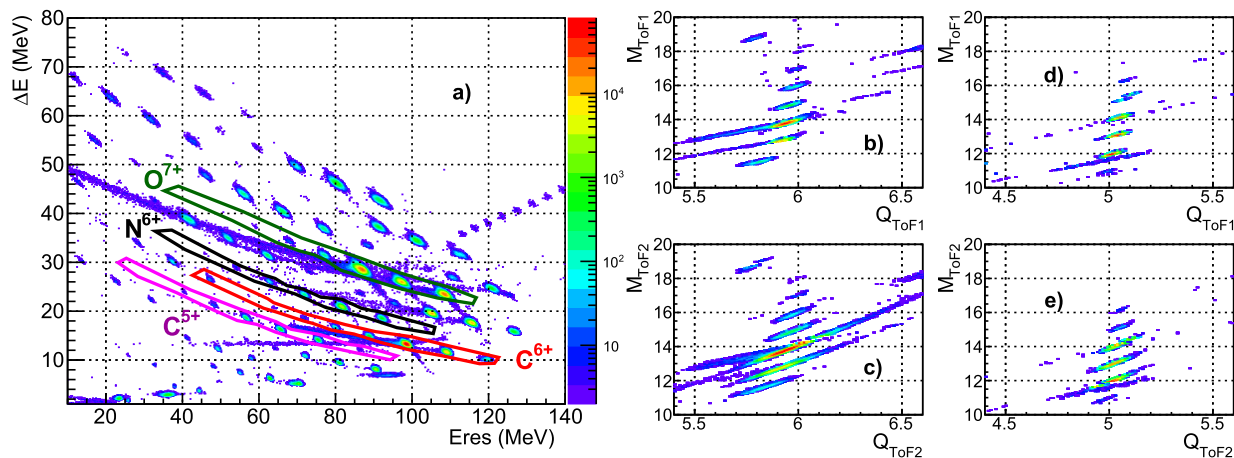


**Fig. 1.** (Color online) Identification plots, number of counts greater than two, obtained at a  $B\rho = 0.9592$  Tm setting for the LISE spectrometer. Panel a) shows a typical  $\Delta E$  vs residual Energy plot measured with the Silicon telescope. The red, black and green contours are examples of selections for the regions of carbon  $6^+$ , nitrogen  $6^+$  and oxygen  $7^+$  charge state, respectively. Loci corresponding to the pile-up of the beam charge states are also visible (dotted diagonal distribution crossing  $E_{res} = 120$  and  $\Delta E = 38$  MeV); for the most intense reaction products, such as  $^{14}\text{C}$ , reactions in the telescope are visible (for example horizontal continuous distribution at  $\Delta E \approx 13$  MeV). Panels b), c) and d), e) present the derived masses for the  $\text{C}^{6+}$  and  $\text{C}^{5+}$  charge state selection, respectively, using the complementary information provided by ToF1 and ToF2 and the total energy information provided by  $\Delta E$  and Eres (see text for details).

tion times during which the system can undergo sizable angular deflections. As a consequence, the maximum of the angular distribution, for products of multi-nucleon transfer processes, moves toward forward angles with the number of nucleons exchanged. Together with the geometrical focusing illustrated in the Wilczynski plot [3], this suggests an enhancement of the production of the exotic reaction products resulting from DIC near or at zero degrees. However, thus far, no experimental information exists on whether this enhancement is actually present.

Until now, measurements of product cross sections at exactly 0 degrees have not been performed for DIC due to hard-to-overcome difficulties in the beam separation at relatively low energy and to the broad transverse momentum distribution of DIC products. Close to 0 degrees DIC measurements can be found in Ref. [7,15].

The issue of predicting the cross sections at 0 degrees for exotic nuclei produced in DIC is of paramount importance in view of the future availability of large-acceptance 0 degrees magnetic spectrometers, such as the S3 facility under construction at GANIL [8], where high-intensity, low-energy heavy-ion beams (5–15 MeV/A) will be used. The selection of DIC exotic products at 0 degrees by such devices could become a method for production of low-energy secondary beams of exotic nuclei.

In the present work, the production of exotic neutron-rich species in DIC is explored for the  $^{18}\text{O} + ^{238}\text{U}$  reaction. The choice of the  $^{238}\text{U}$  target was dictated by it having the highest N/Z ratio among stable isotopes, thus promoting transfers from  $^{18}\text{O}$  towards very neutron-rich nuclei (i.e., east of  $^{18}\text{O}$ ). The measurement was performed at the GANIL facility using the LISE achromatic spectrometer [9]. The experiment employed a 8.5 MeV/A beam of  $^{18}\text{O}^{8+}$  impinging on a  $1 \pm 0.1$  mg/cm $^2$  thick  $^{238}\text{U}$  target, placed in the first object focal point of the LISE spectrometer (D3). The  $^{238}\text{U}$  target was produced at GSI by evaporation on a backing of  $50 \pm 5$   $\mu\text{g}/\text{cm}^2$   $^{nat}\text{C}$ . A  $5 \pm 0.5$   $\mu\text{g}/\text{cm}^2$   $^{nat}\text{C}$  protective layer against oxidation was deposited on the opposite side. The projectile-like products were selected by the spectrometer according to the emission angle and the magnetic rigidity  $B\rho = p/q$  ( $p$  is the momentum of the ion and  $q$  its charge state).

The angular acceptance for the LISE spectrometer is  $\approx 1$  degree with respect to the central trajectory. To minimize the effects of the spectrometer acceptance, only trajectories having the magnetic rigidity close to that of the central trajectory were selected (i.e.,  $\delta p/p < 0.122\%$ ). The identification of the reaction products

was performed with a  $\Delta E$ -E silicon telescope placed in the first image focal plane of the spectrometer (D4). In addition, two time-of-flight values (ToF1, ToF2) were recorded using as the start signal each of the silicon detectors and the radio-frequency of the cyclotron as the stop one. The  $\Delta E$ , E, ToF1 and ToF2 data, together with the  $B\rho$  information given by the settings of the spectrometer, could then be used to extract the mass number A, the atomic number Z and the charge state  $q$  for each detected reaction product. Fig. 1 provides an example of the identification achieved. The  $B\rho$  setting of the spectrometer and the opening of the momentum slits (F31), placed in the first dispersive focal plane of the spectrometer, defined the magnetic rigidity of the selected nuclei. The F31 slits were typically set at  $\pm 2$  mm, knowing that LISE's dispersion is 16.5 mm/% of the momentum bite  $\delta p/p$ . The momentum distribution for the PLF was obtained by performing measurements at different  $B\rho$  settings of the spectrometer. The main experimental challenge consisted in the careful tuning of the spectrometer, avoiding in as much as possible the primary beam charge states to ensure a tolerable counting rate in the silicon detection system. This task was made difficult by the wide charge state distribution and large width of the momentum distribution for each beam charge state. Thus, an intensity between 100 nA and 1  $\mu\text{A}$  was used for each setting. The beam current was measured at the beginning of each run with a calibrated Faraday cup and fluctuations during the run were recorded using a non-interceptive beam profiler (TiD3). In total, 5 different settings for the LISE spectrometer were used: 0.8297, 0.9591, 0.9592, 0.9691, and 1.0904 Tm. To subtract the reactions induced on the  $^{nat}\text{C}$  backing of the target, a separate measurement was performed on a 1 mg/cm $^2$   $^{nat}\text{C}$  target, for each setting. It should be noted that the  $^{18}\text{O} + ^{nat}\text{C}$  reaction contributed to the production of nuclei located up to two neutrons beyond the valley of stability.

The kinetic energy (KE) distributions of the neutron-rich reaction products, obtained by summing the contribution of each charge state, are presented in Fig. 2. Owing to the high beam intensity used (up to 1  $\mu\text{A}$ ), the detection limit was pushed down to  $\approx 10^{-7}$  mb/MeV, enabling the observation of exotic species such as  $^{15}\text{B}$ ,  $^{18,19}\text{C}$ ,  $^{20}\text{N}$ ,  $^{22}\text{O}$ ,  $^{24}\text{F}$  and  $^{25}\text{Ne}$  which survived the strongly dissipative interactions. The KE distributions of these products are broad, thus reflecting a strong energy dissipation, as expected for fragments emitted at very forward angles. The differential reaction cross section at 0 degrees (Fig. 3), was obtained for each product

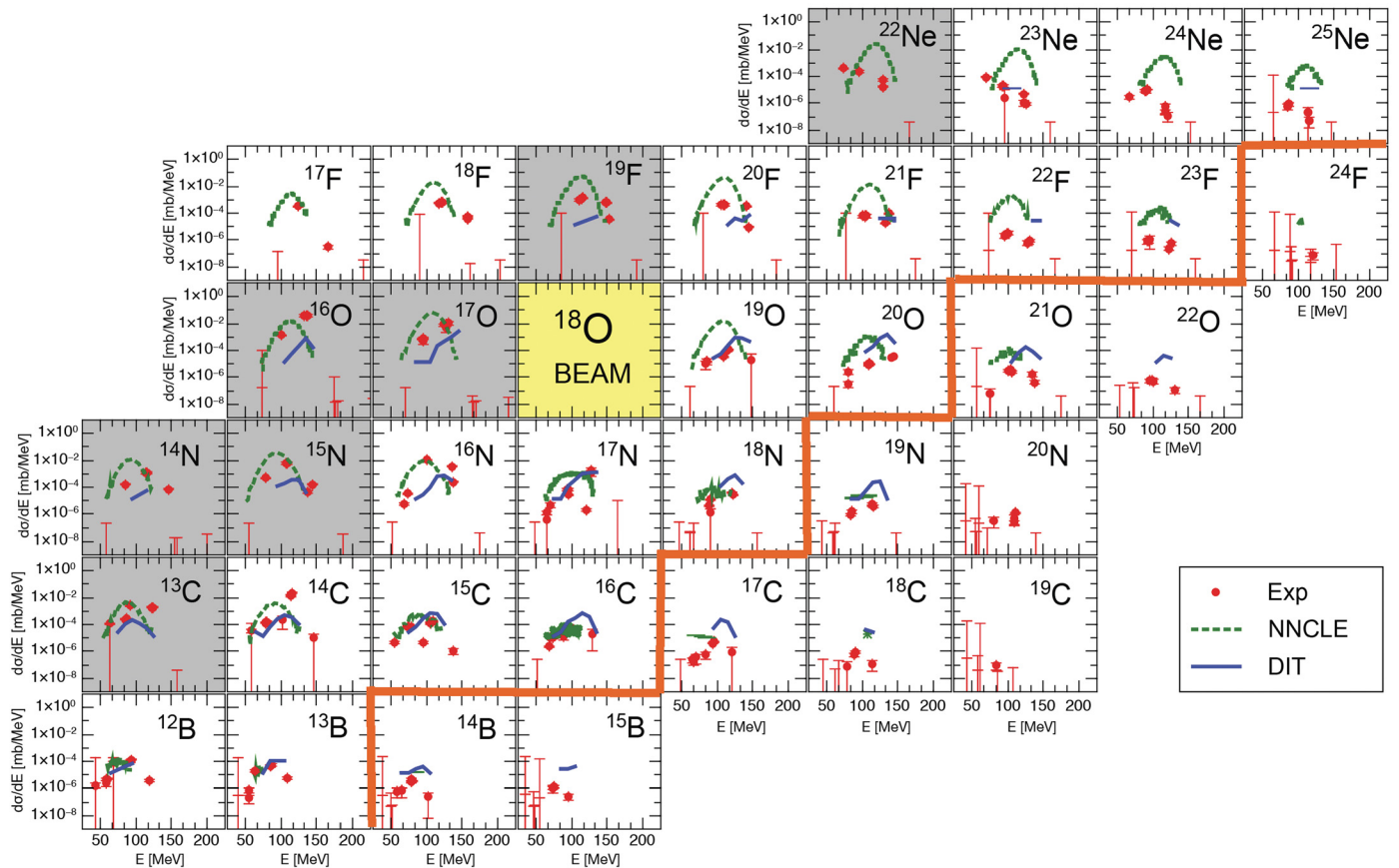


**Fig. 2.** (Color online) Kinetic energy distributions for all identified reaction products obtained from a high-intensity 8.5 MeV/A  $^{18}\text{O}^{8+}$  beam impinging on 1 mg/cm<sup>2</sup> thick  $^{238}\text{U}$  target. The gray boxes represent the stable nuclei, the yellow one is for the beam and white boxes indicate the radioactive nuclei. Red dots represent the experimental reaction cross sections  $d\sigma/dE$  obtained within the LISE acceptance ( $\lesssim 1$  degree), compared with the theoretical calculations – NNCLE coupled with the NRV model (dotted green lines) [16,17], DIT model coupled with Gemini++ (continuous blue lines) [18,19] (see text). The nuclei adjacent to the orange line on the left have the N/Z ratio similar to the  $^{18}\text{O} + ^{238}\text{U}$  system. The major part of the uncertainty arises from the statistical error of each of the points of the momentum distribution, while the error in the momentum acceptance and the angular acceptance of the spectrometer are  $\ll 1\%$  and  $\approx 10\%$ , respectively. The 10% uncertainty in the thickness of the  $^{238}\text{U}$  and  $^{12}\text{C}$  targets was also taken in account.

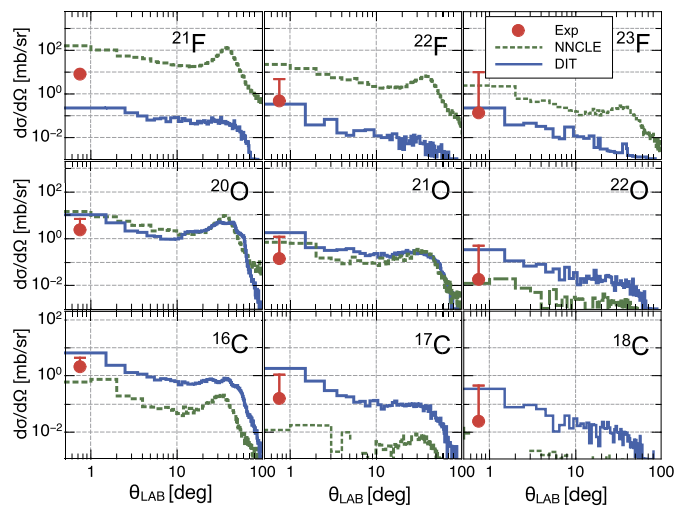


**Fig. 3.** (Color online) Comparison between the data (red) and the results of calculations for selected nuclei. The calculated  $d\sigma/d\Omega$  cross sections as a function of angle are given in green for the NNCLE + NRV model and in blue for DIT + Gemini++ approach (see text for details).

by integrating the KE distributions of Fig. 2. The results are summarized in Table 1.

Prior to this study, very limited experimental information was available in the literature on the production cross sections for fragments formed in DIC processes induced by light-heavy ions (with  $A = 10\text{--}24$ ) on medium-mass or heavy targets [10–13]. Nevertheless, an extended experimental study of the mechanisms of PLF production for low-energy collisions of  $^{14}\text{N}$  on  $^{159}\text{Tb}$  is reported in Refs. [10,11], indicating that, at low collision energies, a dominant contribution to the yields of PLFs heavier than Li is originating from DIC. Indeed, the measured energy distributions of PLFs for that system demonstrate the typical damped mechanism of their formation associated with large dissipation of KE (see the upper panel of Fig. 4 in Ref. [10]). These data were successfully reproduced by the model of Zagrebaev and Greiner [14] which is based on Langevin-type equations of motion. The agreement between data and calculations can be viewed as support for the validity of this approach for the description of DIC induced by light heavy ions.

The experimental results presented here were interpreted on the basis of two different models of DIC, while also taking into account fragment evaporation from the binary collision products: i) the recently developed model of *Nucleus–Nucleus Collisions based on Langevin Equations* (NNCLE) [16], coupled with the NRV statistical code for the description of particle evaporation [17], and ii) the *Deep Inelastic Transport* model (DIT) [18], coupled to the Gemini++ statistical evaporation code [19].

**Table 1**

Differential reaction cross sections  $d\sigma/d\Omega$ , in mb/sr, for the observed nuclei. The values are obtained from the integration of the momentum distribution displayed in Fig. 2 using a linear interpolation and taking into account the LISE spectrometer angular acceptance.

N	5	6	7	8	9	10	11	12	13	14	15	16
Z												
10(Ne)								46 <sup>+6</sup> <sub>-5</sub>	24 <sup>+200</sup> <sub>-3</sub>	.9 <sup>+4</sup> <sub>-1</sub>	.02 <sup>+9</sup>	.001 <sup>+4</sup>
9 (F)				12 <sup>+8</sup> <sub>-2</sub>	50 <sup>+6</sup> <sub>-5</sub>	53 <sup>+5</sup> <sub>-5</sub>	43 <sup>+8</sup> <sub>-4</sub>	7.9 <sup>+1</sup> <sub>-8</sub>	.49 <sup>+2</sup> <sub>-.05</sub>	.13 <sup>+1</sup> <sub>-.02</sub>	.0014 <sup>+.0003</sup> <sub>-.0002</sub>	
8 (O)			1.8 <sup>+4</sup> <sub>-2</sub>	600 <sup>+70</sup> <sub>-60</sub>	420 <sup>+42</sup> <sub>-42</sub>	<b>beam</b>	12 <sup>+3</sup> <sub>-2</sub>	2.5 <sup>+4</sup> <sub>-3</sub>	.14 <sup>+1</sup> <sub>-0.02</sub>	.02 <sup>+5</sup>		
7 (N)			96 <sup>+40</sup> <sub>-10</sub>	290 <sup>+35</sup> <sub>-30</sub>	530 <sup>+300</sup> <sub>-60</sub>	57 <sup>+7</sup> <sub>-6</sub>	1.5 <sup>+8</sup> <sub>-2</sub>	.22 <sup>+9</sup> <sub>-0.03</sub>	.036 <sup>+4</sup> <sub>-.004</sub>			
6 (C)	1.9 <sup>+3</sup> <sub>-2</sub>	110 <sup>+12</sup> <sub>-11</sub>	150 <sup>+17</sup> <sub>-16</sub>	630 <sup>+70</sup> <sub>-65</sub>	7.3 <sup>+8</sup> <sub>-8</sub>	2.2 <sup>+2</sup> <sub>-3</sub>	.16 <sup>+1</sup> <sub>-.02</sub>	.024 <sup>+4</sup> <sub>-.003</sub>	.001 <sup>+4</sup>			
5 (B)	100 <sup>+20</sup> <sub>-15</sub>	58 <sup>+7</sup> <sub>-6</sub>	5.7 <sup>+7</sup> <sub>-6</sub>	1.8 <sup>+2</sup> <sub>-2</sub>	.15 <sup>+03</sup> <sub>-.02</sub>	.029 <sup>+4</sup> <sub>-.003</sub>						

As shown in Fig. 2, the two independent models provide a satisfactory description of the cross sections as a function of the dissipated energy for neutron-rich reaction products with  $Z \leq Z_{beam}$ , including the majority of the exotic ones:  $^{21-22}\text{O}$ ,  $^{17-19}\text{N}$ ,  $^{15-18}\text{C}$ ,  $^{12-15}\text{B}$ . For some of the most exotic products (i.e.,  $^{20}\text{N}$  and  $^{19}\text{C}$ ), the results of the models are not reported, due to the limited statistics obtained with the Monte Carlo calculations. For  $Z > Z_{beam}$ , the experimental data are not well reproduced by the NNCLC calculations (dotted lines) which, in general, overestimate the production of fragments, while the DIT and Gemini++ model (solid lines) gives yields closer to the measurements (when statistical significant Monte Carlo calculations were available).

In order to further examine the characteristics of fragment production at 0 degrees in DIC, the experimental differential cross sections, integrated over the energy distributions of the products (cf. Table 1), have been compared with model predictions for selected reaction fragments:  $^{16-18}\text{C}$ ,  $^{20-22}\text{O}$  and  $^{21-23}\text{F}$ . As seen in Fig. 3, the  $d\sigma/d\Omega$  calculations, performed as a function of the scattering angle, display pronounced maxima at 0 degrees for all the products considered, and the agreement with experiment is noteworthy (within one order of magnitude with the exception of  $^{21}\text{F}$ , where the discrepancy is up to a factor of 30). This result represents the first validation of DIC reaction models at 0 degrees, where the most dissipative component of the reaction mechanism is present. Further, it is found that both models predict a secondary maximum around the grazing angle for less exotic nuclei. In contrast, for the most exotic isotopes, the reaction cross section quickly drops when moving away from 0 degrees to reach vanishingly small values near the grazing angle.

The calculated angular distributions of the cross sections in Fig. 3, together with *i*) the observed experiment-theory agreement discussed above, and *ii*) the fact that the models considered here are known to be reliable for the description of reaction cross sections at larger angles [16,18], indicate that the production of exotic nuclei in DIC at near-barrier energies peaks at 0 degrees.

In summary, this work presents, for the first time, a comprehensive set of experimental data on reaction cross sections for light-heavy exotic nuclei produced in deep-inelastic collisions at 0 degrees. Comparisons with calculations performed with the NNCLC and DIT models indicate that both approaches provide, at this particular angle, a rather satisfactory description of the data for the exotic species. Their production is associated, in particular, with the removal of protons and transfer of neutrons. This represents the first validation of DIC reaction models at 0 degrees, where ge-

ometrical focusing should occur, leading to an enhanced reaction cross section for the projectile-like fragments produced in the dissipative processes. In addition, the measurement is consistent with the prediction, by both models, of reaction differential cross sections being maximal at 0 degrees for the most exotic fragments. This feature may be taken into consideration for the production of exotic beams from DIC products while taking advantage of the zero-degree magnetic spectrometers and high-intensity primary beam accelerators that are currently being developed at several laboratories. The S3 spectrometer at SPIRAL2 at GANIL is an example [8].

The authors thank the technical services of GANIL for providing excellent working condition at the LISE spectrometer. This work was supported in part by the Italian Istituto Nazionale di Fisica Nucleare, by the Polish National Science Centre under Contract No. 2014/14/M/ST2/00738 and 2013/08/M/ST2/00257, by the Russian Science Foundation (17-12-01170) and by the U.S. Department of Energy, Office of Nuclear Physics, under Contract No. DE-AC02-06CH11357 (ANL). One of us (D.A.) was supported by the European Commission in the framework of the CEA-EUROTALENT program.

## References

- [1] W.U. Schroeder, J.R. Huizenga, Damped Nuclear Reactions, in: D.A. Bromley (Ed.), Treatise on Heavy-Ion Science, Springer, N.Y./London, 1985, pp. 113–726.
- [2] R. Kaufmann, R. Wolfgang, Phys. Rev. 121 (1961) 192.
- [3] J. Wilczynski, Phys. Lett. B 47 (1973) 484.
- [4] V.V. Volkov, Phys. Rep. 44 (1978) 93.
- [5] L.G. Moretto, R.P. Schmitt, Rep. Prog. Phys. 44 (1981).
- [6] A. Gobbi, Lecture Notes in Physics, vol. 168, 1982, p. 159.
- [7] G.A. Souliotis, et al., Phys. Rev. C 84 (2011) 064607.
- [8] A. Drouart, J.A. Nolen, H. Savajols, Int. J. Mod. Phys. E 18 (2009) 2160.
- [9] R. Anne, et al., Nucl. Instrum. Methods A 257 (1987) 215.
- [10] G.J. Balster, et al., Nucl. Phys. A 468 (1987) 93.
- [11] G.J. Balster, et al., Nucl. Phys. A 468 (1987) 131.
- [12] G. Benzoni, et al., Eur. Phys. J. A 45 (2010) 287.
- [13] S. Bottoni, et al., Phys. Rev. 85 (2012) 064621.
- [14] V.I. Zagrebaev, W. Greiner, J. Phys. G 34 (2007) 1.
- [15] O.B. Tarasov, Nucl. Phys. A 629 (1998) 605.
- [16] A.V. Karpov, V.V. Saiko, Phys. Rev. C 96 (2017) 024618.
- [17] V.I. Zagrebaev, Y. Aritomo, M.G. Itkis, Yu.Ts. Oganessian, M. Ohta, Phys. Rev. C 65 (2001) 014607; V.I. Zagrebaev, A.V. Karpov, A.S. Denikin, A.P. Alekseev, M.A. Naumenko, V.A. Rachkov, V.V. Samarin, V.V. Saiko, NRV web knowledge base on low-energy nuclear physics, <http://nrvjinnr.ru/>.
- [18] L. Tassan-Got, C. Stéphan, Nucl. Phys. A 524 (1991) 121.
- [19] R.J. Charity, Phys. Rev. C 82 (2010) 014610.